remote sensing

MDPI

Article

Mapping Tropical Forest Cover and Deforestation with Planet NICFI Satellite Images and Deep Learning in Mato Grosso State (Brazil) from 2015 to 2021

Fabien H. Wagner [1,2,3,*], Ricardo Dalagnol [1,2,3], Celso H. L. Silva-Junior [1,2,3], Griffin Carter [1,3], Alison L. Ritz [3,4], Mayumi C. M. Hirye [5], Jean P. H. B. Ometto [6] and Sassan Saatchi [1,2,3]

1 Institute of the Environment and Sustainability, University of California, Los Angeles, CA 90095, USA
2 NASA-Jet Propulsion Laboratory, California Institute of Technology, Pasadena, CA 91105, USA
3 CTREES, Pasadena, CA 91105, USA
4 Interdisciplinary Graduate Education Program in Remote Sensing, Virginia Polytechnic Institute and State University, Blacksburg, VA 24061, USA
5 Quapá Lab, Faculty of Architecture and Urbanism, University of São Paulo—USP, São Paulo 05508-900, Brazil
6 Earth System Sciences Center, National Institute for Space Research—INPE, Sao José dos Campos, São Paulo 12227-010, Brazil
* Correspondence: fhwagner@ucla.edu

Abstract: Monitoring changes in tree cover for assessment of deforestation is a premise for policies to reduce carbon emission in the tropics. Here, a U-net deep learning model was used to map monthly tropical tree cover in the Brazilian state of Mato Grosso between 2015 and 2021 using 5 m spatial resolution Planet NICFI satellite images. The accuracy of the tree cover model was extremely high, with an F1-score >0.98, further confirmed by an independent LiDAR validation showing that 95% of tree cover pixels had a height >5 m while 98% of non-tree cover pixels had a height <5 m. The biannual map of deforestation was then built from the monthly tree cover map. The deforestation map showed relatively consistent agreement with the official deforestation map from Brazil (67.2%) but deviated significantly from Global Forest Change (GFC)'s year of forest loss, showing that our product is closest to the product made by visual interpretation. Finally, we estimated that 14.8% of Mato Grosso's total area had undergone clear-cut logging between 2015 and 2021, and that deforestation was increasing, with December 2021, the last date, being the highest. High-resolution imagery from Planet NICFI in conjunction with deep learning techniques can significantly improve the mapping of deforestation extent in tropical regions.

Keywords: tropical forests; semantic segmentation; U-net; TensorFlow 2; land-cover and land-use

Citation: Wagner, F.H.; Dalagnol, R.; Silva-Junior, C.H.L.; Carter, G.; Ritz, A.L.; Hirye, M.C.M.; Ometto, J.P.H.B.; Saatchi S. Mapping Tropical Forest Cover and Deforestation with Planet NICFI Satellite Images and Deep Learning in Mato Grosso State (Brazil) from 2015 to 2021. *Remote Sens.* **2023**, *15*, 521. https://doi.org/10.3390/rs15020521

Academic Editors: Beatriz M. Funatsu and Sergio Bernardes

Received: 16 November 2022
Revised: 12 January 2023
Accepted: 13 January 2023
Published: 16 January 2023

1. Introduction

Deforestation of tropical forests, caused mainly by expanding forestry and agriculture, is currently the second largest source of anthropogenic carbon emissions, with 5.3 ± 2.4 GtCO2 emitted per year in the period of 2001–2019, and is still increasing [1–5]. In the Brazilian Amazon, the deforestation rate of 2020 was the greatest of the decade so far [6], and was recently surpassed by the 2021 deforestation rate, with 13.032 km^2 [7]. In addition to carbon loss, ∼40% of this deforestation happens in old-growth tropical forests, causing an increase in fragmentation [8] and constituting a direct threat to biodiversity [1]. Monitoring changes in tree cover for the rapid assessment of deforestation is considered the key component of any climate mitigation policy for reducing emissions from deforestation, restoration of forests for biodiversity, and carbon sequestration [9,10].

However, maps of tree cover and deforestation are still challenging datasets to produce. One of the most renowned and accurate products of deforestation monitoring is PRODES from the National Institute of Space Research of Brazil, INPE [11]. Since 1988, PRODES has monitored clear-cut deforestation in the Amazon and produced annual deforestation

rates for the Brazilian government. PRODES defines deforestation as the suppression of areas of old-growth forested physiognomies by anthropogenic actions from intact forest cover to other land use [7]. It is produced based on the visual interpretation of satellite imagery and manual mapping of deforestation by trained specialists over the course of the PRODES year, which starts on August 1st and ends on July 31st [7]. The PRODES map is based on satellite datasets at 20–30 m of spatial resolution and a 5–16 day revisit rate (currently Landsat-8, SENTINEL-2, and CBERS-4/4A). Some pixels have no observation due to high cloud coverage during the course of one year. One of the limits of the product is that manual sampling constrains the time of production of the map and limits the scale of the areas that can be considered as deforested. For example, PRODES does not map deforestation below 6.25 ha [7]. Another major product to monitor deforestation is the 'forest loss year' dataset, a part of the Global Forest Change (GFC) products, the first global map at 30 m of forest cover freely available globally from the University of Maryland [12]. This product looks at the annual change in tree cover in relation to the tree cover of the year 2000 at 30 m spatial resolution globally. Forest loss is defined as the stand-replacement disturbance or the complete removal of tree cover canopy at the Landsat pixel scale. These two products, PRODES and GFC's tree loss year product, are reference datasets to monitor deforestation; however, they are delivered annually and at 30 m of spatial resolution. Furthermore, PRODES is limited to deforested areas above 6.25 ha and GFC's tree loss year product includes forest fires and forest degradation in the tree loss product, not only deforestation. Besides these deforestation products, there exists a large number of methods and data to map or detect deforestation in the tropics [13,14], but here we choose to compare only to the two major products of deforestation publicly available because they are the most used for our study region.

Recently, planet satellite images over the tropics have been made available by Norway's International Climate and Forest Initiative (NICFI) to help save the world's tropical forests while improving the livelihoods of those who live off, in, and near the forests [15,16]. The planet NICFI images are multispectral satellite images containing red, green, blue, and near infrared bands at 4.78 m of spatial resolution for the normalized analytic basemaps. The temporal resolution of the NICFI images is currently one per month, and they are a mosaic composite of the best daily acquisitions during the month. Consequently, planet NICFI images are mostly cloud-free, thus providing the best freely available multispectral dataset to monitor land-use and land-cover (LULC) changes in tropical regions.

However, while planet NICFI images provide the best spatial and temporal resolution to map tropical forest cover with optical data, the variation of reflectance values between the different planet satellite sensors, between dates, and sometimes within the same image is highly challenging. As stated by the NICFI documentation, the absolute radiometric accuracy is not guaranteed for the normalized surface reflectance basemaps [17]. For the non-deep learning remote sensing analysis, where high quality reflectance values are needed, mapping tropical forest cover is almost unfeasible unless several preprocessing steps are made, such as indices creation and bands normalization [18,19]. However, for deep learning methods, high quality or fidelity of reflectance values are not necessary. For example, to recognize cars or plastic balloons in images, convolutional neural network models (CNNs) are even trained with images where the hue is artificially changed (during data augmentation) to impede the model to give too much importance to the color, which could be considered as overfitting in this case [20]. Furthermore, colors (or values in the color channels red, green, and blue) can be seen as one feature when we currently know that several features and multiple levels of abstraction are needed to reach state-of-the-art accuracy of classification [21] as demonstrated by the success of CNNs in computer vision tasks. CNNs correspond exactly to what is needed here, to extract the maximum information relevant to forest mapping using pixel context and not only pixel-based color values with minimal preprocessing from the unequally calibrated images. Furthermore, deep learning has already been applied with success for tasks such as classification of clouds,

shadows, and land-cover scenes in PlanetScope [22] and to map deforestation in Brazil with Landsat images [23,24].

To segment evergreen forest tree cover in planet images, several CNN models were available, such as U-Net, SegNet, FC-DenseNet, or DeepLabv3+, among others [25]. The U-net [26] was chosen because the accuracy of these algorithms is very similar but with simpler architectures, such as U-net, which requires less effort for model training and whose inference is among the fastest [27]. Furthermore, this model has already exhibited excellent performance on tropical forest cover mapping in very high-resolution images [28]. Here, the tree cover model returns a binary value for each pixel, 0 or 1 for non-forest or forest, respectively, that constitutes the tree cover mask. Then, the deforestation date is obtained from the differences of the forest masks at each date. The model was tested in the Mato Grosso state of Brazil with the complete planet dataset from December 2015 to March 2022, corresponding to a total of 77,082 images. The region, located in the south of the Amazon Forest, was chosen because it has overcome large amounts of deforestation in the past. Between the years 2000 and 2013, there has been an estimated 76,360 km^2 of deforestation in Mato Grosso which corresponds to 32% of the total Brazilian Amazon deforestation estimates in that period [29]. Furthermore, Mato Grosso state is located the region known as the "Arc of Deforestation" in the Brazilian Amazon forest and contains some of the main current deforestation fronts.

This work presents (i) the first regional scale mapping of evergreen tree cover and deforestation at a 5 m spatial resolution and a six months temporal resolution using planet NICFI images and deep learning, (ii) the validation of the tree cover product with independent tree cover masks based on planet data and from an independent LiDAR dataset, and (iii) the comparison with PRODES deforestation and GFC's "tree loss year" loss products.

2. Materials and Methods

2.1. Planet Satellite Images of Mato Grosso, Brazil

There were 2658 planet tiles of ∼20 km × 20 km at ∼4.78 m spatial resolution covering the entire Mato Grosso state of Brazil, as seen in Figure 1. This study region represents ∼1 millions of km^2. Images were downloaded through the Planet API [30] and with the PlanetNICFI R package [31] for all the 29 available dates [16] at the time of the study. The complete dataset contained 77,082 planet images with a biannual temporal resolution from 1 December 2015 to1 June 2020 and a monthly temporal resolution from 1 September 2020 to 1 March 2022. All bands in raw image digital numbers (12 bits), red (0.650–0.682 µm), green (0.547–0.585 µm), blue (0.464–0.517 µm), and the NIR bands (0.846–0.888 µm) [32], were, first, truncated to the range of 0–2540 for the RGB bands and scaled between 0 and 2540 for the NIR bands (i.e., divided by 3.937). Second, the 4 bands were scaled to 0–255 (8 bits) by dividing by 10 and then the Red–Green–Blue–NIR (RGBNIR) composite was built. The forest reflectance values are low in the RBG bands (<500) and the specific scaling of these bands was made to optimize the range of values of the forest reflectance in 8 bits. The scaling of NIR is only a min–max (0–10,000) scaling as forest reflectance values are not low in this band. No atmospheric correction was performed. A second image was generated from the composite by adding a mirroring border of 128 pixels on each side for the deep learning prediction in order to remove border effects.

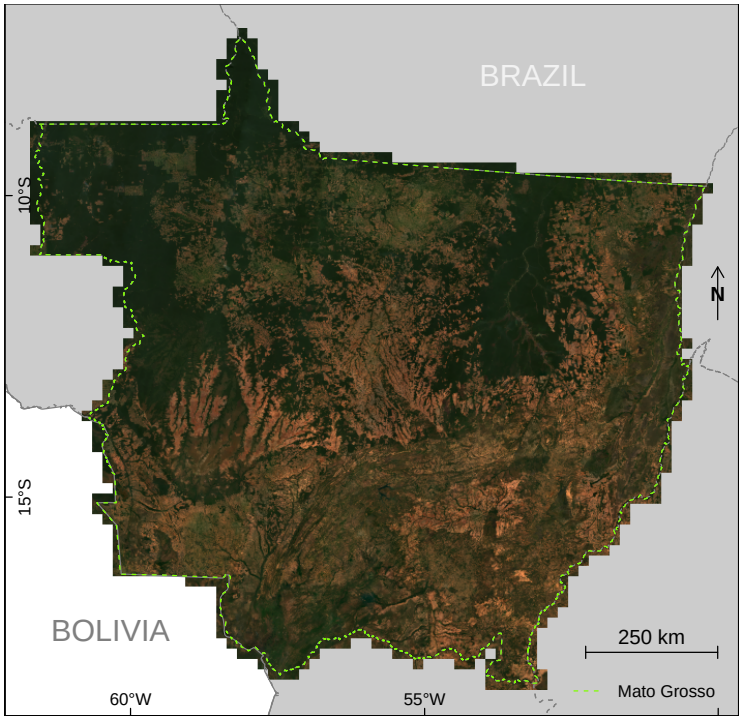

Figure 1. September 2021 planet NICFI mosaic of the Mato Grosso state, Brazil.

2.2. LiDAR Tree Cover Dataset

To validate our tree cover map, we compared our results to the LiDAR height data that were acquired in the scope of the Amazon Biomass Estimate project (EBA/INPE). This dataset is constituted of discrete-return LiDAR data from 610 flight lines of 15 km long by 0.5 km wide distributed randomly over the Amazon region (∼787 ha each; total area of 480,000 ha). The LiDAR dataset was acquired during 2016 using the Trimble HARRIER 68i laser scanning system at an average flight altitude of 600 m. Multiple LiDAR returns were recorded with a minimum point density of 4 points per m^2. The horizontal and vertical accuracy ranged from 0.035 m to 0.185 m and from 0.07 m to 0.33 m, respectively. Among this dataset, we selected 141 flight lines that intersected entirely with the Planet images over Mato Grosso. The LiDAR point clouds were processed into digital terrain models (DTM) and canopy height models (CHM) with 1 × 1 m cell size, as described by [33,34] and the median of the data was aggregated at the resolution of the planet data. Finally, the heights of 49,179,890 planet pixels were available and the height distributions were described in the pixels classified as forest (47,267,739 pixels) and non-forest (1,912,151 pixels).

2.3. Deforestation History Datasets

Our tree cover and deforestation results were compared to two independent deforestation products over the region. The first product is PRODES from INPE [11]. The PRODES project monitors clear-cut deforestation in the Brazilian Legal Amazon based on satellite images of ∼20–30 m of spatial resolution (Landsat-8, CBERS-4, and similar imagery) and delivers official annual rates of forest loss for Brazil (1988–2021). The publicly available annual maps are all corrected/edited manually by experts and contain polygons with the following labels: forest, non-forest, deforestation of the year, previous deforestation, clouds, and water. The minimum area considered for mapping deforestation is 6.25 ha. The second product is the forest loss year component of the Global Forest Change map of the University of Maryland at 30 m spatial resolution based on Landsat data [12,35]. Forest Cover Loss is defined as a stand-replacement disturbance, or a change from a forest to non-forest state, during the period from 2000 to 2021. Both datasets were compared to our product (i) by computing the total area intersecting with our product at each time period, and (ii) by

computing the percentage of intersections of GFC's tree loss year or PRODES with our product by tiles, weighted by the number of observations in GFC or PRODES.

2.4. Neural Network Architecture

The segmentation of evergreen forest cover was made with a classical U-net model [26], as seen in Figure 2. More specifically, the U-net model returns the probability of presence of evergreen tropical forest in each pixel of a given input image. The model inputs are 4 bands of RGB–NIR images made up of 256 × 256 pixels and the output is a mask of one band and 256 × 256 pixels containing 1 (forest cover, pixel probability ≥0.5) or 0 (non-forest, probability <0.5). The model was coded in R language [36] with RStudio interface to Keras and TensorFlow 2.8 [37–40].

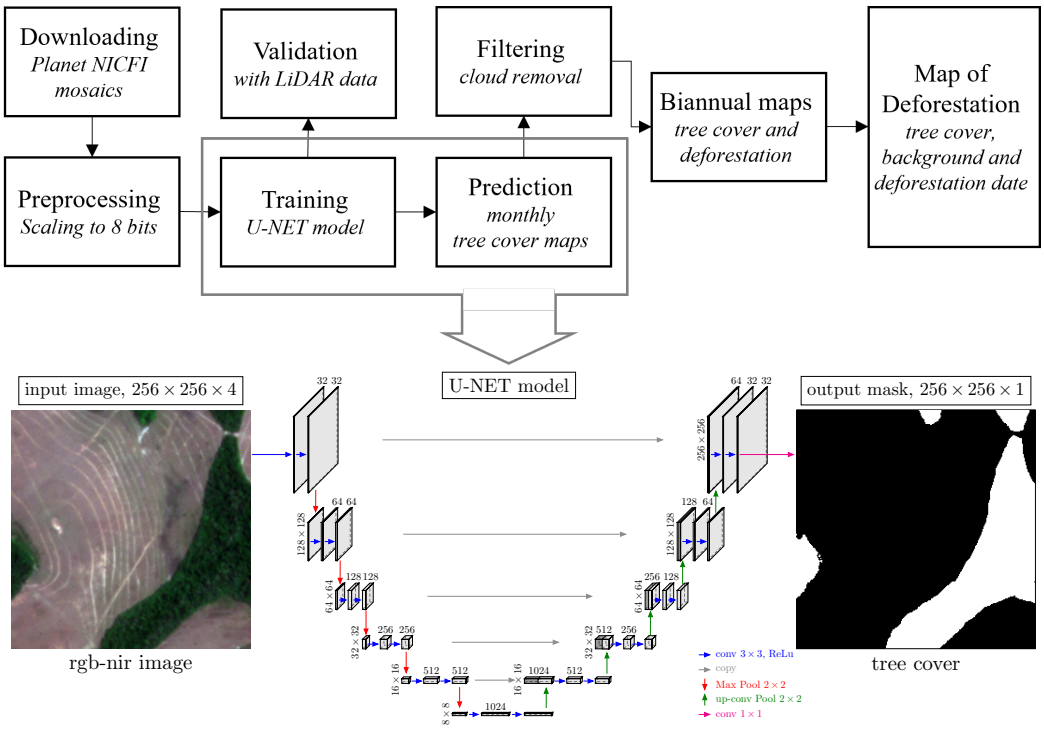

Figure 2. Overall flowchart of the deforestation mapping with planet NICFI and architecture of the U-net model used to produce tree cover masks.

2.5. Training

To produce the training samples of evergreen forest cover for the U-net model, 10 planet images were randomly selected over Mato Grosso for each monthly planet mosaic date from September 2020 to September 2021 inclusive, to constitute a dataset of 130 images. This strategy was used in order to have images for all the seasons and distributed all over Mato Grosso. Among this dataset, 75 images were then selected after removing images with a high cloud cover or large variations in illumination. Then, for the selected images, we ran the k-textures model [41] to perform image self-segmentation with 8 classes. The k-textures is a deep learning-based algorithm which provides self-supervised segmentation of a 4-band image (RGB–NIR) for k number of classes and is designed to ease the production of training samples for satellite image segmentation [41]. After running the k-textures self-segmentation, the user defines which classes found by the algorithm are forest and which are non-forest. After verifying the k-texture results on the 75 images, we kept only 23 images where the forest segmentation was deemed accurate according to the visual interpretation of the forest and non-forest areas. Small errors of the forest mask were manually corrected. At this step, the masks had only two classes: forest (1) and non-forest (0), which contained agriculture, urban area, water surface, and bare ground. From this dataset, we trained a first U-net model [26] and applied prediction of tree cover over the

original 130 images. Then, we removed the 23 images used in the first training sample, and selected a second set of 21 images with atmospheric conditions such as cloud and haze. The forest masks were selected or manually corrected to keep forests with no haze or very thin transparent cloud, while removing all clouds and heavy haze. Here, we want the model to classify clouds and haze as non-forest when forests are difficult to recognize even by the human eye, keeping only the forests that a human can easily recognize as forest cover. From the first and second samples, we constitute a training sample of 6663 images in patches of 256 × 256 pixels and their associated labeled masks for the final U-net model. A total of 6187 images contained forest and background and 476 only background. Of the total images, 80% (5331) were used for training and 20% (1332) for validation.

Each image patch went through a data augmentation process that consisted in random vertical and horizontal flips. No additional data augmentation was necessary due to the natural data augmentation provided by different atmospheric conditions and illumination due the different dates of the sampling images [42]. After data augmentation, the images were then fed to the U-net model.

During network training, we used a standard stochastic gradient descent optimization. The loss function was designed as a sum of two terms: binary cross-entropy and Dice coefficient-related loss of the predicted masks [37,38,43] and finally the optimizer Adam [44] with a learning rate of 0.0001 was used. We used the accuracy (i.e., the frequency with which the prediction matches the observed value) as the metrics to assess the model performance. The network was trained for 20,000 epochs with a batch size of 256 images and the model with the best weighted accuracy was kept for prediction (epoch 17,058 and training/validation accuracy of 99.40 and 97.70%, respectively, and training/validation loss of 0.0088 and 0.0574, respectively). The training of the models took approximately 12.5 h using a Nvidia RTX2080 Graphics Processing Unit (GPU) with an 8 GB memory.

2.6. Prediction

For the prediction of tree cover, a border of 64 neighboring pixels containing a mirroring image was added on each side of the planet tiles of 4096 × 4096 pixels. This border method was used to avoid border artifacts during prediction, a known problem for the U-net algorithm [26]. Then, the prediction of tree cover was made on the entire image and cropped to recover the original 4096 × 4096 pixels planet tiles size. To belong to the evergreen forest class, the pixel prediction value must be greater than or equal to 0.5; otherwise, the pixel is classified as non-forest. The prediction of tree cover for one planet tile took approximately 7 seconds using a Nvidia RTX3090 GPU.

2.7. Cloud Temporal Filtering

Even with the high temporal resolution of planet satellite image acquisition (daily), the monthly mosaic product can still contain some clouds. As clouds are classified as non-forest with a value of 0, keeping them would create false deforestation in the deforestation product. To filter for these clouds, we designed a simple temporal filter. To be classified as an evergreen forested pixel, a pixel at a given date must have been detected as evergreen forest cover for at least half of the observations over the period defined by the closest 3 dates before and after the given date. For the borders of the time series, we used the all the available dates in the ±3 months around the date to filter. All the tree cover masks obtained in prediction were filtered with the temporal filter for cloud removal.

2.8. Tree Cover and Deforestation Biannual Maps

At this step, we considered that the tree cover masks, filtered for clouds, are almost cloud-free and we give only a maximum of two chances for a forest to have been misclassified as non-forest in the 2015–2021 period due to clouds. For example, for one date, if on the period of the cloud filter (±3 months), the forested pixel has never been observed due to clouds, and was consequently classified as non-forest.

Then, we process the time series from the present to the past to reconstruct the deforestation map per pixel. We keep only biannual time series at this point and the produced deforestation map is also biannual. For each pixel at each date, we keep or correct the value of the pixel with rules described in the following text and we attribute a value of trust of the classification: trust = 1 for "confirmed" where the pixel is tree cover or deforestation, trust = 2 for "very likely" where a pixel is classified as tree cover on most of the dates, but classified as non-tree cover on only 1 or 2 dates and with these dates being not the first and the last. Note that the non-forested pixel values are all set to tree cover in this case. Finally, trust = 3 for "unconfirmed". This value of 3 is only for the deforestation of the last available date, to be confirmed with the next available date. Deforestation is defined by a forested pixel at the date $N - 1$ that became classified as non forest at the date N. The data are processed starting from the last date to the first date and the rules are applied at each date. Deforestation is also confirmed during the process when a pixel at $N - 1$ is classified as deforested and still deforested at N. This pixel is confirmed as deforestation and its trust value becomes 1. The result of these steps are corrected tree cover and deforestation masks for all the dates and their associated values of classification confidence. Finally, the biannual deforestation map is created with the following classes: non forest in 2015, forest that has remained forest from 2015 to the last observed date, and the date of deforestation if the pixel was deforested.

3. Results

3.1. Tree Cover Model Validation

The tree cover algorithm presented a high level of segmentation accuracy, with an overall accuracy of 98.11% and an F1-Score of 0.982 (precision = 0.975, recall = 0.988) on the 1332 images patches (256 × 256 pixels) of the validation sample.

An independent validation of our tree cover product was made by comparing the median height measured by LiDAR at 1 m spatial resolution inside the planet pixels overlapping entirely with the 141 EBA LiDAR footprints above Mato Grosso. It represented 47,267,739 pixels for tree cover and 1,912,151 pixels for non-tree cover.

In the non-tree cover pixels classified by U-net, very few pixels have a median high above 2.5 m, as seen in Figure 3a. We found that 94% of the non-tree cover pixels had a value below 0.55 m, 1% in the values ranging between 0.55 m and 2.07 m, 3% in the range between 2.07 m and 4.45 m, and only 2% above 4.45 m. This indicates that classification of non-tree cover is highly accurate and contains very few trees.

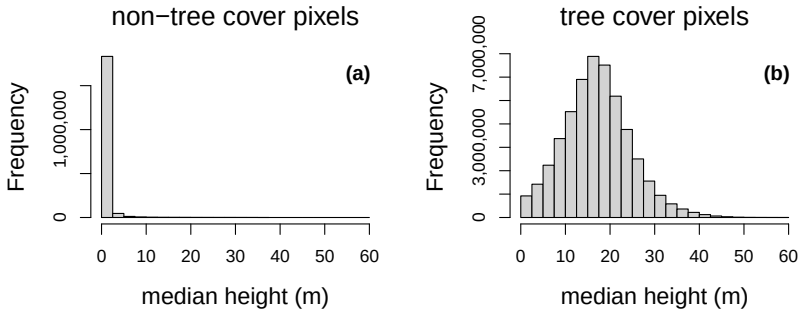

Figure 3. Distribution of median height in the planet pixels that intersects (with full overlap) with 141 EBA LiDAR datasets randomly distributed over Mato Grosso, for planet pixels classified by U-net as non-tree cover (**a**) and tree cover (**b**).

For the tree cover pixels, the height was distributed in a Gaussian shape around the median height of 16.9 m, as seen in Figure 3b, and 5% of the tree cover pixels had median height below 5.02 m. Overall, based on the LiDAR data, it is observed that our tree cover model segment trees with a very high accuracy, that is, 98% of non-forest pixels have a

height below 5 m, and around 95% of the tree cover pixels have a height above 5 m. This indicates that the classification of tree cover is highly accurate, although not as accurate as non-tree cover pixels. However, it is worth noting that forest can also contain some gaps with a height below 5 m.

3.2. Tree Cover and Deforestation of Mato Grosso

For the Mato Grosso state, a tree cover of 556,510.8 km^2 was found for the year 2015, which represents 58.1% of the state's area, as seen in Table 1. Between December 2015 and December 2021, this area was diminished by ∼141,598.5 km^2 (14.8% of the total area of Mato Grosso). The biannual deforestation data did not show a clear seasonal preference for deforestation. After reaching the minimum value of deforestation area in December 2016 with 6632.05 km^2, the biannual deforestation area exhibited a tendency to increase between December 2016 and December 2019 and a sharp increase was observed thereafter, with the deforested area of December 2021 (19,817.8 km^2) being almost double the deforested area of December 2019 (9944.5 km^2). It is worth noting that new forests growing after 2015 are not accounted for in these numbers. Furthermore, even with the 6-months cloud filter, some clouds can remain in the last date, and the results for 1 December 2021 should be taken with caution. Our results show that deforestation is still ongoing and is high in the state of Mato Grosso. At the rate of the tree cover removal we observed between December 2012 and December 2021, it would take less than 20 years to remove all the tree cover that was present in 2015.

Table 1. Tree cover and its change due to deforestation in the period from 1 December 2015 to 1 December 2021 obtained with planet data and the U-net tree cover model.

Classes	Area (km^2)	Area (%)
2015 total tree cover	556,510.76	58.08
2015 non-tree cover	401,689.23	41.92
2015 remaining tree cover	414,912.25	43.30
deforestation June 2016	18,763.20	1.96
deforestation December 2016	6632.05	0.69
deforestation June 2017	8511.05	0.89
deforestation December 2017	8037.00	0.84
deforestation June 2018	8066.52	0.84
deforestation December 2018	9016.48	0.94
deforestation June 2019	8812.72	0.92
deforestation December 2019	9944.50	1.04
deforestation June 2020	9998.04	1.04
deforestation December 2020	15,297.82	1.60
deforestation June 2021	18,701.35	1.95
deforestation December 2021	19,817.78	2.07

Only 52 (1.96 %) of the 2658 planet tiles of Mato Grosso state have less than 1 km^2 of tree cover change in the period between 2015 and 2021, as seen in Figure 4. This shows that deforestation is widespread in the state of Mato Grosso. The mean deforested area was 57.2 km^2 per tiles (the tile area is 382.9019 km^2). A total of 455 tiles (17.1%) exhibit a deforested area above 100 km^2. Some areas with current intensive tree cover change are clustered, such as areas located in the south of Mato Grosso, and near the largest forest remnants.

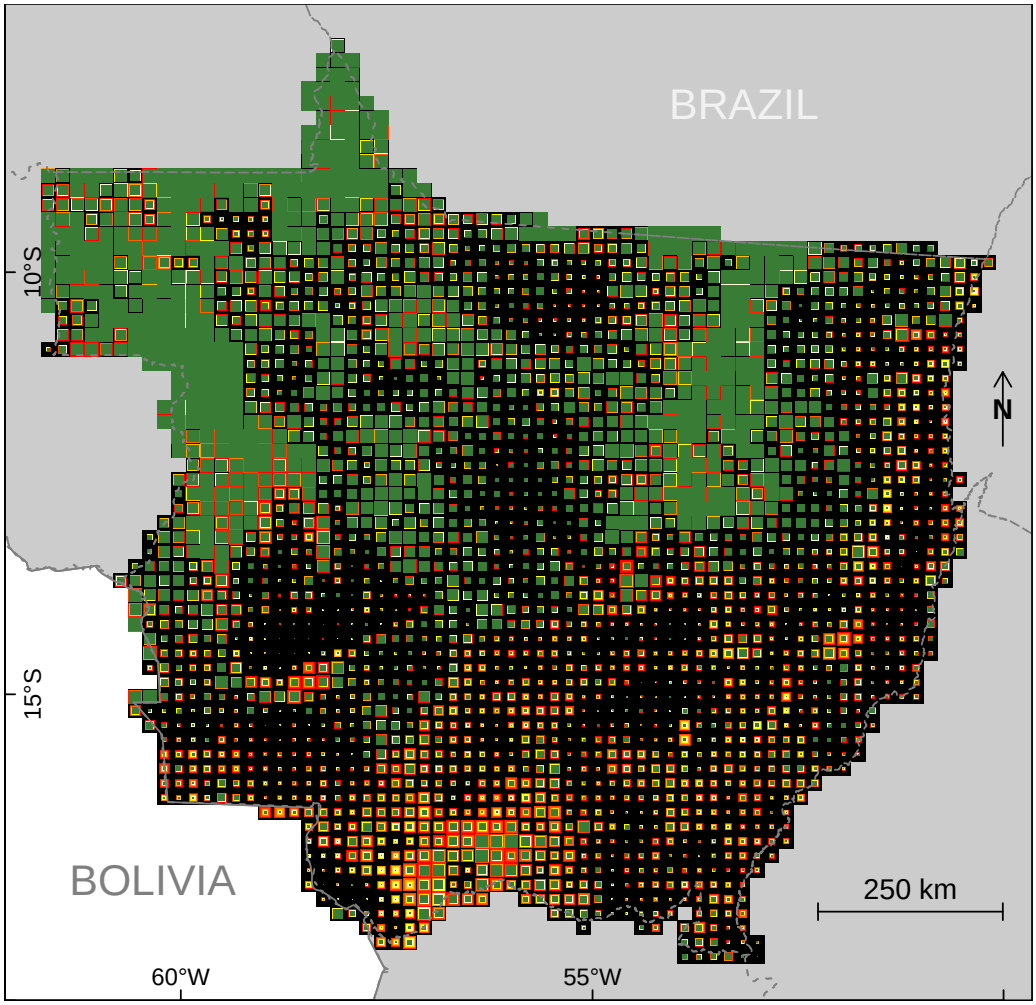

Figure 4. Tree cover and tree cover loss per year for the 2658 planet tiles covering the Mato Grosso state, Brazil, with colored areas representing the real size of tree cover, deforestation, and non-tree cover in each tile. Remaining tree cover of 2015 is in green, and the yellow-to-red color scale represents the deforestation, with red being the more recent.

Large-scale deforestation still appeared in 2021, for example, in the Xingu region, as seen in Figure 5a. It is worth noting that roads built previously for logging appeared in the largest patch. Depending on the size of the rivers inside the forest, it can take some time for them to appear clearly in the images due to satellite view angle, and small rivers can be mapped as deforestation in the first years, such as the river in the bottom right. Gradually advancing smaller-scale deforestation can also be observed in the Xingu region, as seen in Figure 5b, accompanied by new roads inside the forests. Large-scale deforestation is visible in the recent deforestation front between the Mato Grosso and Amazonas states, as seen in Figure 5c. Some isolated dots are logging decks or roads and indicate where deforestation will likely appear in the near future. An unusual circular pattern of deforestation for Mato Grosso shows active deforestation in 2021, as seen in Figure 5d. It is located in the deforestation front between the Mato Grosso and Amazonas states. Some pattern of tree cover change can be natural or not, for example, in the South Central region of Mato Grosso, as seen in Figure 5e. Natural changes in river border were mapped as deforestation and this region also presents new roads, and large areas of tree cover change. For this region, the large deforestation could be linked to the change from biannual to monthly time series and inclusion as forest when they are deciduous and now observed as deforestation. Note that not all of this deforestation is necessarily illegal. However, for most of these images, small new roads or logging decks located inside the forest can be observed, indicating that logging is active and planned to continue.

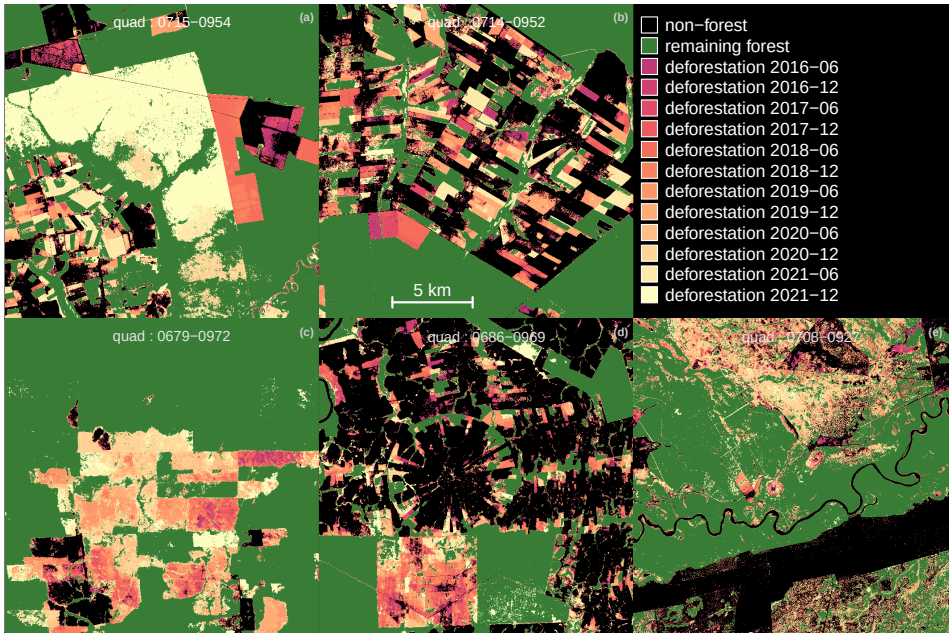

Figure 5. Example of our deforestation product for planet quads in the Xingu region (**a**,**b**), in a recent deforestation front between the Mato Grosso and Amazonas states (**c**,**d**) and in the South Central region of Mato Grosso (**e**) on the period from 1 December 2015 to 1 December 2021.

3.3. Comparison between our Deforestation Product and the Deforestation Estimated by PRODES and GFC Products

In this section, we detail which deforested pixels detected by PRODES or GFC's "tree loss year" are found or not by our product for the Legal Amazon region of the Mato Grosso state.

For the tree cover change in the Amazon for region of Mato Grosso, seen in Table 2, we found more tree cover changes than the PRODES and GFC "tree loss year" products. We found between 3.39 and 7.49 times more deforestation than PRODES depending on the date and the largest discrepancies were found on the last date of our time series. We found between 0.71 and 3.49 times the deforestation from GFC's "tree loss year" product, with the last date having the largest differences. This is expected as our product has a spatial resolution of 4.77 m, while the minimum area for mapping deforestation is 30 m for GFC and 6.25 ha for PRODES. It is worth noting that, even with the 6-months cloud filter, some clouds can remain for the last date of our product, so the results for 1 December 2021 should be taken with caution.

Table 2. Annual tree cover change in the Amazonian region of Mato Grosso in km^2 on the period from 2016 to 1 December 2021 obtained with our product, PRODES, data and GFC "tree loss year" data.

	Our Product (km^2)	Deforestation Prodes (km^2)	GFC Tree Loss Year (km^2)
2016	7762.19	1370.87	5192.88
2017	5453.75	1327.95	7638.69
2018	5959.05	1407.31	3950.39
2019	6271.88	1848.54	3666.78
2020	7638.07	1817.41	5636.31
2021	13,930.53	1860.23	3987.56

Due to the ±3 dates aggregation for cloud filtering, our deforestation data start to be consistent in time with PRODES only when monthly planet data are available. On the period from June 2020 to December 2021, our model intersects with 72.5% of the PRODES data for the year 2021, as seen in Table 3. On the period from June 2019 to June 2021, our

model intersects with 64.4% of the PRODES data for the year 2020. On the period from June 2018 to June 2020, our model intersects with 60.7% of the PRODES data for the year 2019. The largest class outside the intersection of dates is always forest cover, meaning that we have classified as tree cover a pixel that was classified as deforested by PRODES. These can be errors from our model or small patches of forests that are present in the 30 m pixels classified as deforestation by PRODES. These results indicate that even with a different resolution, our deep learning model and PRODES, which is manually edited, have more than half of the deforestation areas in common. This is what we want here, a model that is close to the human interpretation of deforestation in images.

Table 3. Intersection in percentage of annual PRODES data and our bi-annual deforestation product.

			PRODES					
	Non-Forest	**Forest**	**Deforestation December 2016**	**Deforestation December 2017**	**Deforestation December 2018**	**Deforestation December 2019**	**Deforestation December 2020**	**Deforestation December 2021**
OURS								
non-forest	67.30	1.30	52.60	22.20	9.30	6.00	5.00	3.50
forest	19.50	95.30	8.60	9.90	13.60	11.60	17.90	17.20
deforestation								
June 2016	2.10	0.20	8.00	15.50	3.00	1.40	1.10	0.60
December 2016	0.70	0.10	1.90	1.70	0.50	0.40	0.30	0.20
June 2017	0.90	0.10	4.40	13.60	4.20	1.40	0.80	0.50
December 2017	0.80	0.10	3.30	9.80	13.40	2.40	1.00	0.50
June 2018	0.90	0.10	3.10	5.30	16.80	4.20	1.50	0.60
December 2018	0.90	0.10	3.80	4.60	11.40	18.70	2.70	0.90
June 2019	0.80	0.10	3.20	3.20	7.70	18.60	7.20	1.40
December 2019	0.90	0.20	2.70	3.30	5.00	12.50	19.80	2.10
June 2020	0.80	0.20	1.90	2.70	3.20	6.70	16.30	3.60
December 2020	1.20	0.40	2.70	3.40	5.50	7.40	11.80	20.20
June 2021	1.60	0.50	2.10	2.70	3.90	5.50	9.30	34.00
December 2021	1.50	1.40	1.70	2.10	2.70	3.30	5.50	14.70

In the period from June 2020-06 to December 2021, our model intersects with 57.9% of the GFC's "tree loss year" data, as seen in Table 4; with 33.9% in the period from June 2019 to June 2021; and with 36.7% in the period from June 2018 to June 2020. The largest class is always forest cover, meaning that we have classified as tree cover a pixel that was classified as tree loss in GFC data. These are errors from our model and are also expected because GFC's "tree loss year" considers a change inside the Landsat pixels, but this does not always represent a clear-cut of the forest in the pixel, only a significant change in tree cover. Some large fires in Mato Grosso are classified as deforestation in the GFC product, which is not the case in our product, and may also explain the differences.

Table 4. Intersection in percentage of annual GFC tree loss data and our bi-annual deforestation product.

			GFC Tree Loss Year					
	Non Forest	**Forest 2000**	**Deforestation December 2016**	**Deforestation December 2017**	**Deforestation December 2018**	**Deforestation December 2019**	**Deforestation December 2020**	**Deforestation December 2021**
OURS								
non forest	26.90	72.90	26.30	7.80	5.40	4.90	3.90	5.30
forest	67.40	13.10	42.30	50.30	38.70	36.50	56.40	31.60
deforestation								
June 2016	0.80	2.70	5.40	5.30	2.20	1.10	0.60	0.90
December 2016	0.30	0.70	1.20	0.70	0.30	0.60	0.30	0.40
June 2017	0.30	1.20	2.70	4.60	2.80	0.90	0.40	0.50
December 2017	0.30	1.00	2.20	5.00	5.30	1.40	0.40	0.60
June 2018	0.30	1.00	1.90	3.10	9.00	1.90	0.50	0.70
December 2018	0.30	1.20	2.50	3.10	9.20	8.90	0.90	0.60
June 2019	0.30	1.00	2.20	2.60	5.90	11.40	1.50	0.60
December 2019	0.30	1.00	2.30	2.50	4.50	9.40	6.00	0.80
June 2020	0.40	0.70	1.70	2.20	2.90	5.10	7.00	1.00
December 2020	0.50	1.10	2.80	4.30	5.10	6.00	13.50	6.20
June 2021	0.80	1.30	2.60	3.90	4.20	6.00	5.90	21.80
December 2021	1.20	1.20	3.70	4.50	4.40	6.00	2.70	28.90

For the year 2020, the histogram of the percentage of intersection per quad for our product and the PRODES deforestation data shows that our product shares consistent information with the PRODES data, as seen in Figure 6a. The median intersection of PRODES with our product was 67.2%, as 75% of the pixels had more than 50.9% of intersection and 25% had more than 81.7%. It is worth noting that the PRODES data are manually made with data at a 20–30 m spatial resolution and do not consider deforested areas below 6.25 ha. This confirms that our deep learning estimations of deforestation overlap well with

the deforestation estimates made by human visual interpretation (PRODES). Our product shows less agreement with the GFC "tree loss year" data, as seen in Figure 6b. In 2020, only 25% of our data had an intersection above 54%. An important proportion of the GFC tree loss data of 2020 shows almost no intersection with our product as shown by the median of intersection of 27.5%. Still, for some quads, the intersections can be above 80%, as seen in Figure 6b. This could be linked to other events of tree cover change classified as deforestation by GFC, such as fires, and also to a different definition of tree cover change, which is based on the automatic detection of Landsat pixel reflectance change in GFC.

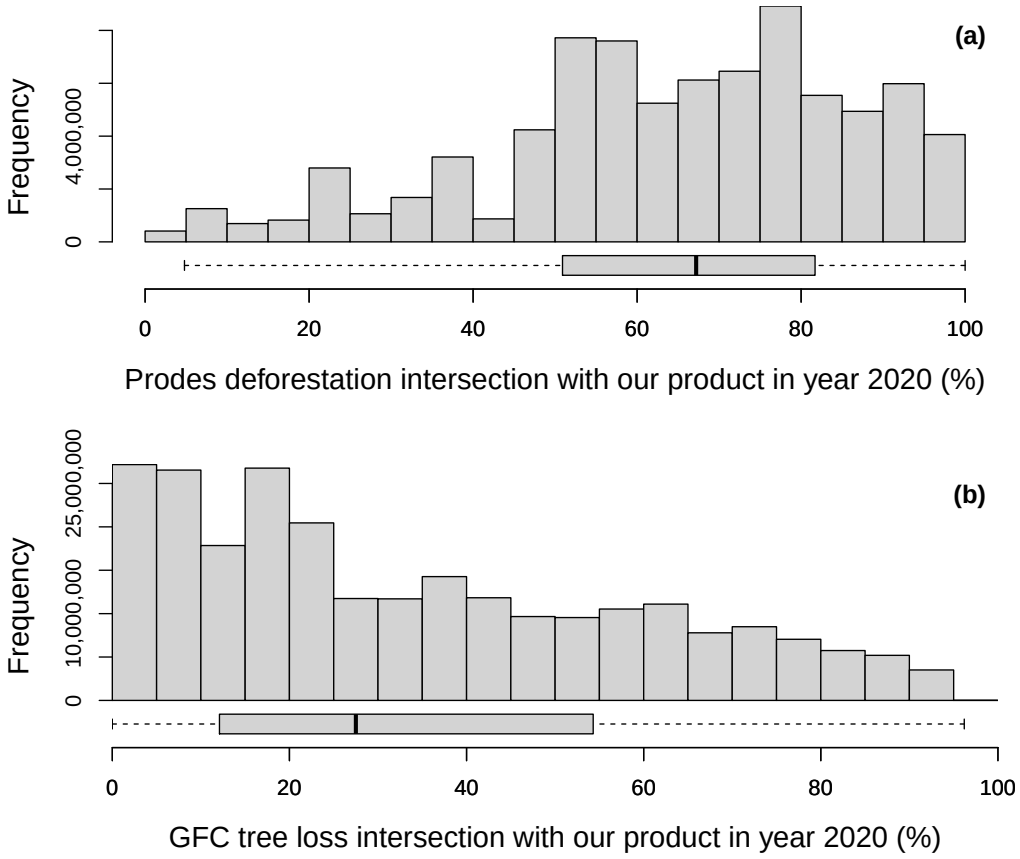

Figure 6. Histogram of intersection per planet tiles of our product of deforestation with the PRODES data (**a**) and GFC tree cover loss (**b**) per quad for the year 2020. Each intersection value was weighed by the number of pixels with intersection observed in the tile, of PRODES or of GFC "tree loss year data". The boxplot of the distribution of intersection is presented below each histogram for the visualization of median and quartiles.

3.4. Comparison between our Deforestation Product and the Deforestation Estimated by PRODES and GFC Products for Some Selected Planet Tiles

For the tiles with similar results with our deforestation map, that is, with more than 90% of intersection between our deforestation mapping and the PRODES or GFC "tree loss year" data, as seen in Figure 7, several observations can be made. Between PRODES and our deforestation data, as seen in Figure 7a,b for the images and in Figure 7e,f for the deforestation masks, it can be observed that PRODES (as expected by the PRODES methodology) included non-forest pixels that are captured by our algorithm with planet images at 5 m such as the logging decks. It can also be observed that our algorithm detected deforested pixels on the borders of the forest patches and roads. This indicates that the pixel attribution has changed; however, it remains difficult to conclude whether this is due to real change in tree cover or due to the imprecise georeferencing of planet

images between the two dates. Between GFC's "tree loss year" data and our product, as seen in Figure 7c,d for the images and in Figure 7g,h for the deforestation masks, it can be observed that GFC's "tree loss year" data produced large patches and also detected some roads, while our product detected many more changes in pixels. Inside deforestation patches, sometimes trees remain, and our algorithm still detects them as forests. Overall, PRODES and GFC's "tree loss year" data give more homogeneous surfaces, while our product, with its finer spatial resolution, gives tree cover at the scale of the tree. Even small gaps in the canopy can be marked as non-forest or few remaining trees inside a deforested patch can be recognized as tree cover. Outside the forest, the change in attribution of our product is difficult to interpret, likely due to deforestation or to the imprecise georeferencing of planet images.

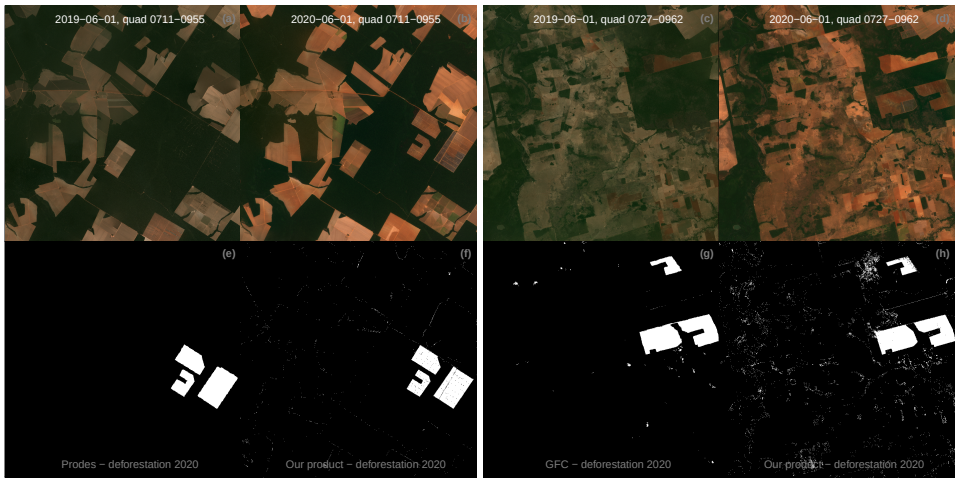

Figure 7. Example of good agreement, i.e., >90% of intersection, of our product of deforestation with the PRODES data (planet quad 0711-0955) and of our product and GFC's "tree loss year" data (planet quad 0727-0962) for the year 2020. Planet NICFI quad is ∼19.5 × 19.5 km.

For the tiles with bad agreement between our deforestation mapping and the PRODES or GFC "tree loss year" data, that is, with less than 10% of intersection, as seen in Figure 8, fire mapped as deforestation in PRODES and in GFC's "tree loss year" data seems to be the culprit, while our algorithm mapped almost no change for the quad 0717-0961 in 2020, as seen in Figure 8a,b,e,f, and a large area of forest that had burned is delineated as deforestation in PRODES, while it is still forest. The same observation is made for the GFC data for the region of the quad 0701-0948 in 2020, as seen in Figure 8c,d,g,h. In this tile, large fires have been mapped as deforestation, while the forest is still there. These fires included in the mapping of deforestation in PRODES or GFC "tree loss year" data leads to a major discrepancy with our product.

For the tiles that show the most extreme difference, that is, our product finds many more pixels than PRODES or GFC's "tree loss year" data (>100,000 pixels), as seen in Figure 9, it can be observed that the changes are mainly isolated pixels. It is also common around rivers and on the border of forests, where our algorithm can pick up very small changes as the spatial resolution is 5 m. However, it remains difficult to say whether it is an anthropic or natural change or even a referencing problem. This also seems to happen for short forest stands that are not highly packed.

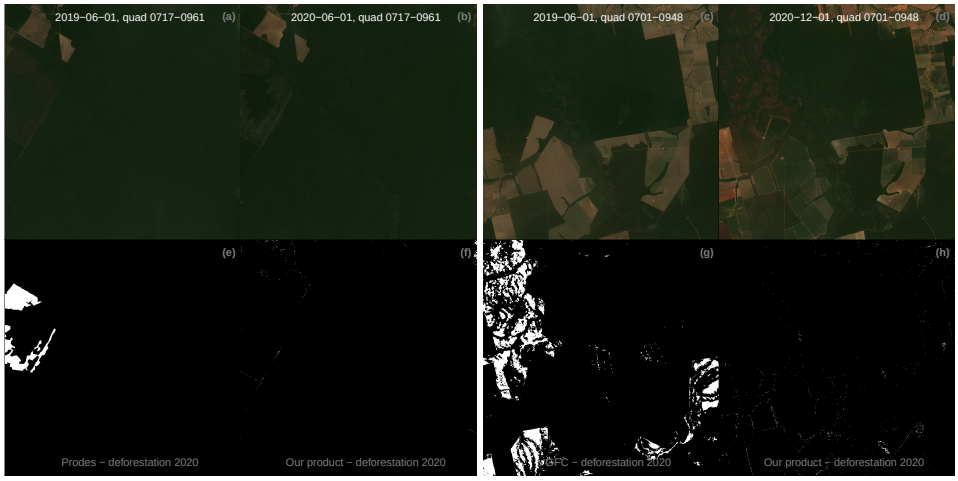

Figure 8. Example of poor agreement, i.e., <10% of intersection, of our deforestation product and the PRODES data (planet quad 0717-0961) and GFC "tree loss year" data (planet quad 0701-09948) for the year 2020. Planet NICFI quad is ∼19.5 × 19.5 km.

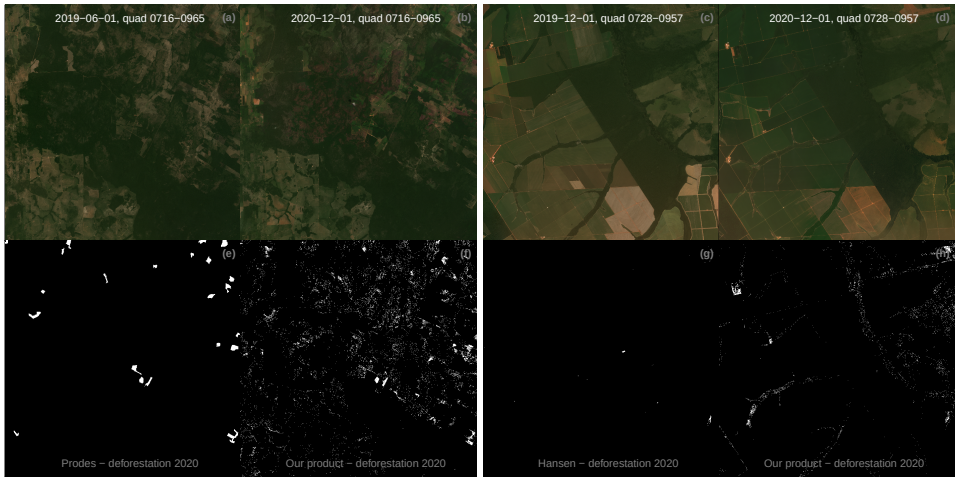

Figure 9. Worst cases of non-agreement between PRODES data (planet quad 0716-0965), Hansen tree cover loss (planet quad 0728-0957), and our product, i.e., <10% of intersection, for the year 2020. Planet NICFI quad is ∼ 19.5 × 19.5 km.

Comparing the deforestation time series between our product, GFC's "tree loss year" data, and the PRODES product, it can be observed that our product tends to delay the timing of deforestation for the first years of the time series, even if it spatially detected these areas well. This is due to the cloud filter that considers three dates around each date to filter for clouds. For example, for the year 2015, the three next dates are 1 June 2016, 1 December 2016, and 1 June 2017 for the cloud filter. This issue is resolved after 1 December 2020, as the first date of the monthly time series is 1 September 2020 and will not appear for the future dates. For the last periods, our product is well aligned with PRODES and GFC's "tree loss year" data and "tree loss year" dataset. Our product appears to be noisier due to the temporal resolution (6 months) as well as the spatial resolution (5 m) while PRODES and GFC's "tree loss year" data produce a more homogeneous area. With our product, it is possible to see deforestation every 6 months. Due to the fact that our product does not use expert interpretation, the results are fast to produce. The time depends only on the release of the image. The deforestation of the end of 2021 is included in our dataset, as it is for GFC's "tree loss year" data but not in PRODES data (PRODES year ends in August, while our study was conducted in May). Our product missed some small regions, mainly due to remaining trees. If some trees are remaining, our model still considers that a forest

is present, while at a 30 m resolution the change of signal between the two dates must be very high and easy to detect. Overall, our results seem to indicate that the time series of deforestation can be obtained with the planet data, at least when the planet time series is monthly.

4. Discussion

4.1. Mapping Evergreen Tropical Forests with Planet NICFI Images and Deep Learning

In the state of Mato Grosso, Brazil, the U-net network identified evergreen tropical forests with an overall accuracy and a F1-score above 98% on the validation dataset, showing again the high capacity of deep learning to support vegetation mapping [25] even in tropical environments [28,45]. In 2015, tree cover represented 58.1% of the state. We found that 43.3% of Mato Grosso in 2021 is still forested with forest that was present in 2015. It is worth noting that our model does not account for regrowing forest. The high performance of the segmentation could be explained by the unique spectral values and textural information of the dense forests when considering the context, for example, as seen in Figures 7–10. The k-textures model that is used to make the training sample was previously shown to segment these forests by textures without human supervision, which further confirms that they contain unique feature characteristics [41]. Here, the accuracy shows the robustness and generalization of the U-net model to such a segmentation task. No heavy preprocessing was used, only a scaling to have 8 bit-images and a border added with mirroring image to avoid the border effect during the prediction. This minimal preprocessing eased the processing of large image databases, such as the database of 77,082 images used here. Planet images have high spectral variability due to the lack of inter-sensor calibration between satellites, as well as the intra-annual variation of sunlight and atmospheric conditions present in the daily imagery that are combined to make the monthly or bi-annual composites [32]. As only a light data augmentation was used, the generalization of the model seems to confirm that natural variation of reflectance present in the satellite images is sufficient to improve the accuracy of the model and to help the model to generalize [42]. Our model was very robust to estimate non-forest as shown by the independent validation with LiDAR data, as seen in Figure 3a, and made only few false positive errors (∼5%) on the forest cover, as seen in Figure 3b. We are less preoccupied by false positives than false negatives, that is, we do not want to miss any forested pixels. False positives can be easily corrected later with the temporal filter. For example, with a simple rule, i.e., the forest attribution cannot change from forest to non-forest and to forest again. Relatively few other observed errors were mainly sparse trees and with a dark green background. As our algorithm looks at the context, if there are still some trees, it can be classified as a forest, and as it does not look at the change between dates, the model is unaware of the diminution in the number of trees and can miss the detection. This is a rare case and is more related to degradation than to deforestation. Predicting the tree cover at each date independently of the other dates is a major difference with models such as GFC map [12], where the authors looked at the difference between dates to identify change. In future work, the deep learning model with planet NICFI images could be adapted to work with the times series, such as works made to detect deforestation with Landsat [23,24], and to account for more subtle change in tree cover. Our method differs from PRODES and GFC on the spatial resolution, temporal resolution, and scaling. In the GCF product approach with Landsat, the spatial resolution is 30 m and, and, in PRODES, no deforestation with an area below 6.25 is mapped [7,12]. Here, our method can map whether a pixel contains a forest or not, 0 or 1, at the 5 m planet NICFI spatial resolution. Furthermore, by using the cloud-free mosaics of planet NICFI, our method enables us to provide an accurate map of the deforestation every 6 months. This differs from PRODES, which is updated annually (but its monitoring year runs from August 1 to July 31) and also from GCF, which is annual [7,12]. Our methods could help monitor deforestation in tropical forested regions of the world, such as Gabon in Africa, where there are more clouds than in the Amazon and the number of Landsat available scenes is from very low to

null [46], but where monthly planet NICFI images are available. Finally, in comparison to a manual product, the scaling of our method is feasible and wall-to-wall, that is, technically, applying our method to another region is just a matter of selecting another region of interest and all processes run automatically to make the deforestation map. As the tree cover is initially self-segmented by the k-textures algorithm, an expert only defines which classes found by the k-textures algorithm are representing tree cover, it is still a challenge to relate our tree cover meaning to the official forest definitions such as the FAO definition: "Land spanning more than 0.5 hectares with trees higher than 5 m and a canopy cover of more than 10 percent, or trees able to reach these thresholds in situ. It does not include land that is predominantly under agricultural or urban land use" [47]. The U-net model needs a lot of data to train, and we still do not dispose of sufficient LiDAR datasets to attempt to get closer to the official definition. In the future, this could be achieved by training a U-net including the height from LiDAR, for example. We acknowledge that the U-net model is not necessarily the best method to produce vegetation/land cover mapping larger than the scale used here, as it would need GPU cloud computing and storage that can come with a high cost. Furthermore, other works using mainly Landsat images and non-deep learning methods [12,48] also exhibit high performance and can cover larger areas. However, in the case of a study using planet images, as the scale of a region or a state, we recommend producing the vegetation class model with U-net. First, because U-net demonstrated high performance for this task such as in this study; second, because it enables the fast and consistent production of monthly tree masks at a 5 m resolution even with the large variation of reflectance in planet NICFI images; and finally, because U-net is relatively easy and convenient to use.

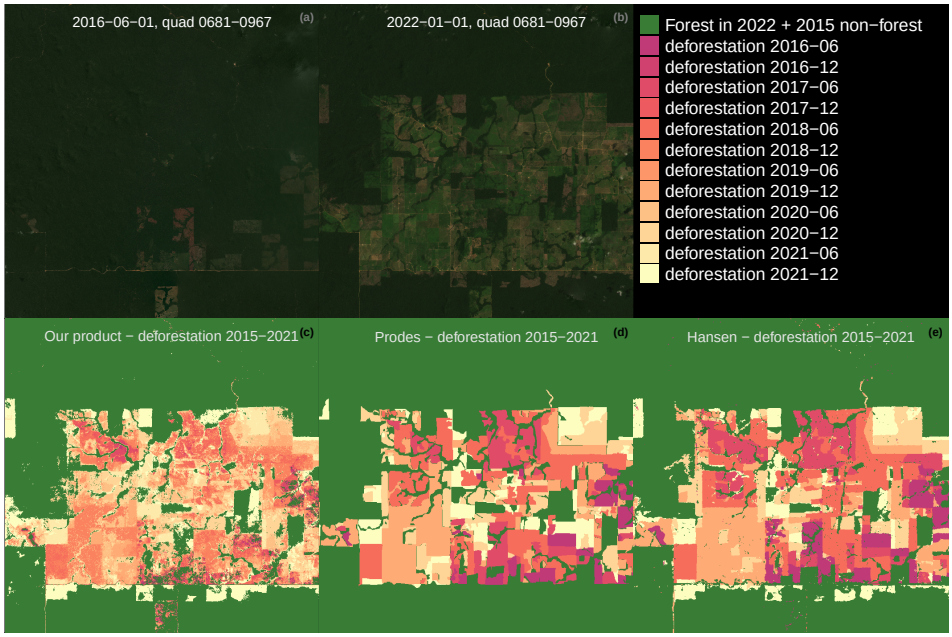

Figure 10. Change in tree cover for the Planet Nicfi quad 0681-0967 localized in Mato Grosso (**a**,**b**). Comparison of our product of deforestation (**c**) with the PRODES data (**d**) and GFC "tree loss year" (**e**) for this quad and for the period from 1 December 2015 to 1 December 2021. Planet NICFI quad is ∼19.5 × 19.5 km.

4.2. The Deforestation of Mato Grosso

The tree cover maps at a very high accuracy for all planet dates enabled the reconstruction of the history of deforestation for the region in the period of 2015–2021 at a spatial resolution of ∼5 m and temporal resolution of 6 months. We observed that deforestation is still widespread in Mato Grosso and the deforestation fronts are active, as seen in Figure 4. Our numbers show that deforestation is still increasing at an alarming rate in this state, with the tree cover change for the second semester of 2021 representing ∼2%

(19,817.78 km^2) of the size of the state, as seen in Table 2. Several types of tree cover changes were observed, from small-scale deforestation to large-scale deforestation, roads, and also natural changes such as changes in river paths, as seen in Figure 5. The deforestation observed in Mato Grosso is likely mainly related to agricultural expansion and logging. Mato Grosso is a major agricultural and livestock production region and deforestation has been previously detected with PRODES in properties currently producing soy and beef [49]. Deforestation is also caused by both legal and illegal logging activity, e.g., in 2018 the state of Mato Grosso produced 53% of the total timber wood extracted from the Brazilian Amazon Forest [50]. One of the major differences with GFC tree cover loss year and PRODES products [11,12] is that the entire tree cover is mapped at each date and not only the change in relation to a fixed previous year (2000 in the case of the GFC map) or previous dataset (deforested areas for PRODES) so we can compute the actual deforestation number. Our product is also biannual where other products are annual, and in the next version we will integrate a cloud mask specific to planet NICFI images to have a monthly product. Large areas mapped by PRODES or GFC's "tree loss year" that were not found by our product were mainly linked to forest fire or degradation due to fire mapped as deforestation, as seen in Figure 8. We considered as tree cover pixels that were classified as tree cover on half of the dates on a moving window of ±three months. Consequently, it is possible that vegetation that is leafless during drought months starts to be detected only with the monthly dataset (since 1 September 2020) and be classified as deforestation, which could increase the detection for the first years of the monthly dataset. This artifact should be resolved with a longer monthly time series. Furthermore, rivers, roads, and clear-cut boundaries are also mapped with increased accuracy during the time series as it can take some time to see them clearly due to minor errors in the co-registration and the satellite view angles of images at different dates [19]. For example, a river can appear as deforestation for the first dates of the series, until the larger path of the river is mapped. This artifact should be resolved with more monthly data. The monthly time series is still very new and some more months would be needed to properly calibrate the deforestation map. Furthermore, our map also accounts for natural changes in tree cover, and not all changes that we observe are human-made tree cover changes. This can explain, in addition to the spatial resolution of 5 m, why our model maps up to 7.49 times more change in tree cover than the 30 m products, as seen in Table 2. In future work, we will also include regrowing forests, as there is a significant amount of regrowing forests and they are very interesting for carbon sequestration, with the potential of contributing 5.5% to Brazil's 2030 net emissions reduction target [51–53]. As for other tropical forest-monitoring systems based on optical imagery, our model can still be limited in areas with high cloud cover and for the fast detection of deforestation, and for early warning systems, radar monitoring could be preferred as they are now efficient and used such as DETER-SAR in Brazil [14]. In future work, we will adapt the methodology to radar images to circumvent the cloud cover issues. Besides supporting forest monitoring and carbon assessment, our 5 m resolution tree cover map could also support forest fragmentation analysis for conservation as forest fragmentation is currently increasing in the Amazon [8,54,55]. Finally, our work demonstrates the potential of deep learning for mapping deforestation with planet NICFI images.

4.3. Perspectives on Training Sample Production for Tree Cover Classification

Here, we used an alternative to produce the large training sample needed to parameterize the U-net model, which is usually done by hand. The production of our training sample was made in a large part automatically with the use of self-segmentation by the k-textures algorithm [41]. The k-textures algorithm provides self-supervised segmentation of an image in a k number of texture classes and is fully deep learning-based. The manual steps in this process consisted of the choice of number of classes returned by the k-textures model, to identify which classes represented forest, to perform small corrections on the mapped results, and to find additional samples of atmospheric conditions, such as forests below

thin clouds which do not need segmentation (only adding in the sample 256 × 256 images with thin cloud cover over forest). The training sample was therefore produced with minimal human supervision, that is, without the need of manually mapping samples of pixels that belonged to the forest class. This enables users to make the training sample very rapidly, in a couple of days, and which could explain the high accuracy of the segmentation. Furthermore, the k-textures already use several features and multiple levels of abstraction, to separate each class, and a human cannot be as consistent and fast [56]. Drawing polygons manually cannot be as accurate as the model, as the manual delineation of pixels cannot follow the pixels in the borders of forests accurately. As a result, the production of the samples was faster and the training sample more accurate. More generally, this approach could ease the production of training samples for classes that have a different texture from other land-covers.

5. Conclusions

In this study, we produced a deep learning-based method to automatically map tree cover and deforestation in the Amazon Forest with planet NICFI images. The accuracy of the tree cover model, demonstrated by the F1-score > 0.98 and the LiDAR validation, made it possible to produce extremely accurate monthly maps of tree cover at 5 m of spatial resolution. From these monthly maps, we produced the biannual deforestation maps after filtering for remaining clouds. These deforestation maps were shown to be close to the manual estimates made by PRODES, which is a general objective of this work, replacing the laborious and time-consuming manual mapping of deforestation with a method that requires only minimal human supervision and which is faster, consistent, and scalable. In our case, only 7 seconds are needed to map an area of 20 km × 20 km. Furthermore, the spatial and temporal resolution of the maps are increased. Regarding the deforestation numbers, for the Mato Grosso state, we observed that 14.8 % of the area covered by forests in 2015 has undergone clear-cut logging. Furthermore, after remaining stable for the period between June 2016 and June 2020, the deforestation started to increase again to reach its maximum in the last measured date (December 2021) with an area equivalent to 2% of the Mato Grosso state. These numbers show the urgency for models, such as the one developed here, to map accurately and rapidly the deforestation in the Amazon and in the other tropical forests to help the reduction in tropical forest deforestation.

Author Contributions: Conceptualization, F.H.W. and S.S.; methodology, F.H.W., R.D., C.H.L.S.-J., G.C., A.L.R. and M.C.M.H.; software, F.H.W. and R.D.; validation, F.H.W., R.D. and J.P.H.B.O.; formal analysis, F.H.W.; investigation, F.H.W., R.D. and S.S.; resources, S.S.; data curation, F.H.W.; writing—original draft preparation, F.H.W., R.D., C.H.L.S.-J. and S.S.; writing—review and editing, F.H.W., R.D., C.H.L.S.-J. and S.S.; visualization, F.H.W.; supervision, S.S.; project administration, S.S.; funding acquisition, S.S. All authors have read and agreed to the published version of the manuscript.

Funding: This research received no external funding.

Data Availability Statement: Planet NICFI data are freely available trough the Planet Mosaics API https://developers.planet.com/docs/basemaps/reference/#tag/Basemaps-and-Mosaics.

Acknowledgments: We thank the team from the EBA project for supporting the use of the airborne LiDAR datasets. Part of this work was carried out at the Jet Propulsion Laboratory, California Institute of Technology, under a contract with the National Aeronautics and Space Administration (NASA). The authors wish to the thank the Grantham Foundation and High Tide Foundation for their generous gift to UCLA and support to CTrees.org.

Conflicts of Interest: The authors declare no conflict of interest. The funders had no role in the design of the study; in the collection, analyses, or interpretation of data; in the writing of the manuscript; or in the decision to publish the results.

References

1. Harris, N.L.; Gibbs, D.A.; Baccini, A.; Birdsey, R.A.; De Bruin, S.; Farina, M.; Fatoyinbo, L.; Hansen, M.C.; Herold, M.; Houghton, R.A.; et al. Global maps of twenty-first century forest carbon fluxes. *Nat. Clim. Chang.* **2021**, *11*, 234–240. [CrossRef]
2. Friedlingstein, P.; Jones, M.W.; O'Sullivan, M.; Andrew, R.M.; Bakker, D.C.; Hauck, J.; Le Quéré, C.; Peters, G.P.; Peters, W.; Pongratz, J.; et al. Global carbon budget 2021. *Earth Syst. Sci. Data* **2022**, *14*, 1917–2005. [CrossRef]
3. Feng, Y.; Zeng, Z.; Searchinger, T.D.; Ziegler, A.D.; Wu, J.; Wang, D.; He, X.; Elsen, P.R.; Ciais, P.; Xu, R.; et al. Doubling of annual forest carbon loss over the tropics during the early twenty-first century. *Nat. Sustain.* **2022**, *5*, 444–451. [CrossRef]
4. Shukla, P.; Skea, J.; Slade, R.; Khourdajie, A.A.; van Diemen, R.; McCollum, D.; Pathak, M.; Some, S.; Vyas, P.; Fradera, R.; et al. (Eds.) *IPCC, 2022: Climate Change 2022: Mitigation of Climate Change. Working Group III contribution to the Sixth Assessment Report of the Intergovernmental Panel on Climate Change*; Cambridge University Press: Cambridge, UK; New York, NY, USA, 2022. [CrossRef]
5. Pendrill, F.; Persson, U.M.; Godar, J.; Kastner, T.; Moran, D.; Schmidt, S.; Wood, R. Agricultural and forestry trade drives large share of tropical deforestation emissions. *Glob. Environ. Chang.* **2019**, *56*, 1–10. [CrossRef]
6. Silva Junior, C.H.; Pessoa, A.; Carvalho, N.S.; Reis, J.B.; Anderson, L.O.; Aragão, L.E. The Brazilian Amazon deforestation rate in 2020 is the greatest of the decade. *Nat. Ecol. Evol.* **2021**, *5*, 144–145. [CrossRef]
7. de Almeida, C.A.; Maurano, L.E.P.; de Morisson Valeriano, D.; Camara, G.; Vinhas, L.; Gomes, A.R.; Monteiro, A.M.V.; de Almeida Souza, A.A.; Rennó, C.D.; Silva, D.E.; et al. Methodology for Forest Monitoring used in PRODES and DETER Projects. *CEP* **2021**, *12*, 010.
8. Montibeller, B.; Kmoch, A.; Virro, H.; Mander, Ü.; Uuemaa, E. Increasing fragmentation of forest cover in Brazil's Legal Amazon from 2001 to 2017. *Sci. Rep.* **2020**, *10*, 5803. [CrossRef]
9. Valeriano, D.M.; Mello, E.M.; Moreira, J.C.; Shimabukuro, Y.E.; Duarte, V.; Souza, I.; Santos, J.; Barbosa, C.C.; Souza, R. Monitoring tropical forest from space: The PRODES digital project. *Int. Arch. Photogramm. Remote Sens. Spat. Inf. Sci.* **2004**, *35*, 272–274.
10. Mitchard, E.T. The tropical forest carbon cycle and climate change. *Nature* **2018**, *559*, 527–534. [CrossRef]
11. National Institute for Space Research (INPE). Monitoring of the Brazilian Amazonian Forest by Satellite. Technical Report, INPE, 1988–2021. Available online: https://www.gov.br/inpe/pt-br (accessed on 15 January 2023).
12. Hansen, M.C.; Potapov, P.V.; Moore, R.; Hancher, M.; Turubanova, S.A.; Tyukavina, A.; Thau, D.; Stehman, S.V.; Goetz, S.J.; Loveland, T.R.; et al. High-Resolution Global Maps of 21st-Century Forest Cover Change. *Science* **2013**, *342*, 850–853. [CrossRef]
13. Pacheco-Pascagaza, A.M.; Gou, Y.; Louis, V.; Roberts, J.F.; Rodríguez-Veiga, P.; da Conceição Bispo, P.; Espírito-Santo, F.D.; Robb, C.; Upton, C.; Galindo, G.; et al. Near real-time change detection system using Sentinel-2 and machine learning: A test for Mexican and Colombian forests. *Remote Sens.* **2022**, *14*, 707. [CrossRef]
14. Doblas, J.; Reis, M.S.; Belluzzo, A.P.; Quadros, C.B.; Moraes, D.R.V.; Almeida, C.A.; Maurano, L.E.P.; Carvalho, A.F.A.; Sant'Anna, S.J.S.; Shimabukuro, Y.E. DETER-R: An Operational Near-Real Time Tropical Forest Disturbance Warning System Based on Sentinel-1 Time Series Analysis. *Remote Sens.* **2022**, *14*, 3658. [CrossRef]
15. Norway's International Climate and Forest Initiative. NICFI. Available online: https://www.nicfi.no/ (accessed on 10 January 2023).
16. Planet Team. Planet Application Program Interface: In Space for Life on Earth. 2017. Available online: https://api.planet.com (accessed on 10 January 2023).
17. Pandey, P.; Kington, J.; Kanwar, A.; Curdoglo, M. Addendum to Planet Basemaps. Product Specifications. NICFI Basemaps. v02. *NICFI Basemaps*, 2021. Available online: https://assets.planet.com/docs/NICFI_Basemap_Spec_Addendum.pdf (accessed on 10 January 2023).
18. Cheng, Y.; Vrieling, A.; Fava, F.; Meroni, M.; Marshall, M.; Gachoki, S. Phenology of short vegetation cycles in a Kenyan rangeland from PlanetScope and Sentinel-2. *Remote Sens. Environ.* **2020**, *248*, 112004. [CrossRef]
19. Francini, S.; McRoberts, R.E.; Giannetti, F.; Mencucci, M.; Marchetti, M.; Scarascia Mugnozza, G.; Chirici, G. Near-real time forest change detection using PlanetScope imagery. *Eur. J. Remote Sens.* **2020**, *53*, 233–244. [CrossRef]
20. Chollet, F.; Allaire, J. *Deep Learning with R*; Manning Publications Co.: Shelter Island, NY, USA, 2018.
21. LeCun, Y.; Bengio, Y.; Hinton, G. Deep learning. *Nature* **2015**, *521*, 436–444. [CrossRef]
22. Shendryk, Y.; Rist, Y.; Ticehurst, C.; Thorburn, P. Deep learning for multi-modal classification of cloud, shadow and land cover scenes in PlanetScope and Sentinel-2 imagery. *ISPRS J. Photogramm. Remote Sens.* **2019**, *157*, 124–136. [CrossRef]
23. Matosak, B.M.; Fonseca, L.M.G.; Taquary, E.C.; Maretto, R.V.; Bendini, H.d.N.; Adami, M. Mapping Deforestation in Cerrado Based on Hybrid Deep Learning Architecture and Medium Spatial Resolution Satellite Time Series. *Remote Sens.* **2022**, *14*, 209. [CrossRef]
24. Maretto, R.V.; Fonseca, L.M.; Jacobs, N.; Körting, T.S.; Bendini, H.N.; Parente, L.L. Spatio-temporal deep learning approach to map deforestation in amazon rainforest. *IEEE Geosci. Remote Sens. Lett.* **2020**, *18*, 771–775. [CrossRef]
25. Kattenborn, T.; Leitloff, J.; Schiefer, F.; Hinz, S. Review on Convolutional Neural Networks (CNN) in vegetation remote sensing. *ISPRS J. Photogramm. Remote Sens.* **2021**, *173*, 24–49. . [CrossRef]
26. Ronneberger, O.; Fischer, P.; Brox, T. U-Net: Convolutional Networks for Biomedical Image Segmentation. *arXiv* **2015**, arXiv:1505.04597.
27. Lobo Torres, D.; Queiroz Feitosa, R.; Nigri Happ, P.; Elena Cué La Rosa, L.; Marcato Junior, J.; Martins, J.; Olã Bressan, P.; Gonçalves, W.N.; Liesenberg, V. Applying Fully Convolutional Architectures for Semantic Segmentation of a Single Tree Species in Urban Environment on High Resolution UAV Optical Imagery. *Sensors* **2020**, *20*, 563. [CrossRef]

28. Wagner, F.H.; Sanchez, A.; Tarabalka, Y.; Lotte, R.G.; Ferreira, M.P.; Aidar, M.P.M.; Gloor, E.; Phillips, O.L.; Aragão, L.E.O.C. Using the U-net convolutional network to map forest types and disturbance in the Atlantic rainforest with very high resolution images. *Remote Sens. Ecol. Conserv.* **2019**, *5*, 360–375. [CrossRef]
29. Tyukavina, A.; Hansen, M.C.; Potapov, P.V.; Stehman, S.V.; Smith-Rodriguez, K.; Okpa, C.; Aguilar, R. Types and rates of forest disturbance in Brazilian Legal Amazon, 2000–2013. *Sci. Adv.* **2017**, *3*, e1601047. [CrossRef] [PubMed]
30. Planet API, NICFI Basemaps. Available online: https://api.planet.com/basemaps/v1/mosaics (accessed on 10 January 2023).
31. Mouselimis, L. *PlanetNICFI: Processing of the 'Planet NICFI' Satellite Imagery Using R*, R package version 1.0.4; 2022. Available online: https://cran.r-project.org/web/packages/PlanetNICFI/index.html (accessed on 10 January 2023).
32. Planet. *Planet Imagery Product Specifications*; Planet Labs: San Francisco, CA, USA, 2021; p. 91.
33. Dalagnol, R.; Phillips, O.L.; Gloor, E.; Galvão, L.S.; Wagner, F.H.; Locks, C.J.; Aragão, L.E. Quantifying canopy tree loss and gap recovery in tropical forests under low-intensity logging using VHR satellite imagery and airborne LiDAR. *Remote Sens.* **2019**, *11*, 817. [CrossRef]
34. Dalagnol, R.; Wagner, F.H.; Galvão, L.S.; Streher, A.S.; Phillips, O.L.; Gloor, E.; Pugh, T.A.; Ometto, J.P.; Aragão, L.E. Large-scale variations in the dynamics of Amazon forest canopy gaps from airborne lidar data and opportunities for tree mortality estimates. *Sci. Rep.* **2021**, *11*, 138. [CrossRef]
35. Hansen Global Forest Change v1.9 (2000–2021). Available online: https://developers.google.com/earth-engine/datasets/catalog/UMD_hansen_global_forest_change_2021_v1_9 (accessed on 15 June 2022).
36. R Core Team. *R: A Language and Environment for Statistical Computing*; R Foundation for Statistical Computing: Vienna, Austria, 2016.
37. Chollet, F. Keras. 2015. Available online: https://github.com/fchollet/keras (accessed on 10 January 2023).
38. Allaire, J.; Chollet, F. *keras: R Interface to 'Keras'*, R Package Version 2.1.4; 2016. Available online: https://cran.r-project.org/web/packages/keras/index.html (accessed on 10 January 2023).
39. Allaire, J.; Tang, Y. *tensorflow: R Interface to 'TensorFlow'*, R Package Version 2.2.0; 2020. Available online: https://cran.r-project.org/web/packages/tensorflow/index.html (accessed on 10 January 2023).
40. Abadi, M.; Agarwal, A.; Barham, P.; Brevdo, E.; Chen, Z.; Citro, C.; Corrado, G.S.; Davis, A.; Dean, J.; Devin, M.; et al. TensorFlow: Large-Scale Machine Learning on Heterogeneous Systems. 2015. Available online: tensorflow.org (accessed on 10 January 2023).
41. Wagner, F.H.; Dalagnol, R.; Sánchez, A.H.; Hirye, M.C.M.; Favrichon, S.; Lee, J.H.; Mauceri, S.; Yang, Y.; Saatchi, S. K-textures, a self-supervised hard clustering deep learning algorithm for satellite image segmentation. *Front. Environ. Sci.* **2022**, *10*, 946729. Available online: https://www.frontiersin.org/articles/10.3389/fenvs.2022.946729 (accessed on 10 January 2023). [CrossRef]
42. Wagner, F.H. The flowering of Atlantic Forest Pleroma trees. *Sci. Rep.* **2021**, *11*, 1–20. [CrossRef] [PubMed]
43. Dice, L.R. Measures of the amount of ecologic association between species. *Ecology* **1945**, *26*, 297–302. [CrossRef]
44. Kingma, D.P.; Ba, J. Adam: A Method for Stochastic Optimization. *arXiv* **2014**, arXiv:1412.6980. https://doi.org/10.48550/ARXIV.1412.6980.
45. Wagner, F.H.; Sanchez, A.; Aidar, M.P.; Rochelle, A.L.; Tarabalka, Y.; Fonseca, M.G.; Phillips, O.L.; Gloor, E.; Aragao, L.E. Mapping Atlantic rainforest degradation and regeneration history with indicator species using convolutional network. *PLoS ONE* **2020**, *15*, e0229448. [CrossRef]
46. USGS. Landsat Global Archive Consolidation. Available online: https://www.usgs.gov/landsat-missions/landsat-global-archive-consolidation (accessed on 10 January 2023).
47. FAO. Global Forest Resources Assessment 2020: Main report. Technical report, Food and Agriculture Organization of the United Nations, ROME. 2020. Available online: https://doi.org/10.4060/ca9825en (accessed on 1 June 2022). [CrossRef]
48. MapBiomas. Project MapBiomas, Collection 2.3 of Brazilian Land Cover & Use Map Series. Technical Report. Available online: https://mapbiomas.org/ (accessed on 9 May 2018).
49. Rajão, R.; Soares-Filho, B.; Nunes, F.; Börner, J.; Machado, L.; Assis, D.; Oliveira, A.; Pinto, L.; Ribeiro, V.; Rausch, L.; et al. The rotten apples of Brazil's agribusiness. *Science* **2020**, *369*, 246–248. [CrossRef] [PubMed]
50. Silgueiro, V.; Cardoso, B.; Vadiones, A.; Batista, L.; Bernasconi, P. *Logging Illegality in Mato Grosso, Brazil, from 2018 to 2019;* Technical Report; Instituto Centro de Vida (ICV): Alta Floresta, MT, Brazil, 2021.
51. Silva Junior, C.H.; Heinrich, V.H.; Freire, A.T.; Broggio, I.S.; Rosan, T.M.; Doblas, J.; Anderson, L.O.; Rousseau, G.X.; Shimabukuro, Y.E.; Silva, C.A.; et al. Benchmark maps of 33 years of secondary forest age for Brazil. *Sci. Data* **2020**, *7*, 269. [CrossRef] [PubMed]
52. Heinrich, V.H.; Dalagnol, R.; Cassol, H.L.; Rosan, T.M.; de Almeida, C.T.; Silva Junior, C.H.; Campanharo, W.A.; House, J.I.; Sitch, S.; Hales, T.C.; et al. Large carbon sink potential of secondary forests in the Brazilian Amazon to mitigate climate change. *Nat. Commun.* **2021**, *12*, 1785. [CrossRef]
53. Rosan, T.M.; Aragao, L.E.; Oliveras, I.; Phillips, O.L.; Malhi, Y.; Gloor, E.; Wagner, F.H. Extensive 21st-century woody encroachment in South America's savanna. *Geophys. Res. Lett.* **2019**, *46*, 6594–6603. [CrossRef]
54. Vogt, P.; Ferrari, J.R.; Lookingbill, T.R.; Gardner, R.H.; Riitters, K.H.; Ostapowicz, K. Mapping functional connectivity. *Ecol. Indic.* **2009**, *9*, 64–71. [CrossRef]

55. Strassburg, B.B.; Barros, F.S.; Crouzeilles, R.; Iribarrem, A.; Santos, J.S.d.; Silva, D.; Sansevero, J.B.; Alves-Pinto, H.N.; Feltran-Barbieri, R.; Latawiec, A.E. The role of natural regeneration to ecosystem services provision and habitat availability: A case study in the Brazilian Atlantic Forest. *Biotropica* **2016**, *48*, 890–899. [CrossRef]
56. Brodrick, P.G.; Davies, A.B.; Asner, G.P. Uncovering Ecological Patterns with Convolutional Neural Networks. *Trends Ecol. Evol.* **2019**, *34*, 734–745. [CrossRef] [PubMed]